Nanoscale Contacts between Carbon Nanotubes and Metallic Pads

Ning Peng, Hong Li, and Qing Zhang*

Microelectronics Center, School of Electrical and Electronic Engineering, Nanyang Technological University 639798, Singapore

ARTICLE

ABSTRACT It is well-known that the electrical properties and performance of carbon nanotube field-effect transistors (CNTFETs) are largely dominated by their nanotube/metal contacts. Such nanometer-scaled contacts are typically different from traditional bulk semiconductor/metal contacts, as a thin layer of molecules could be unintentionally introduced between the CNTs and metal electrodes through either adsorption of environmental molecules or device fabrication processes. Here, we present a nanocontact model, in which the energy band bending in the CNTs near the contacts is quantitatively characterized through establishment of electrostatic charge balance between the CNTs and metallic pads under the influences of environmental oxygen. The concept of dipole polarization along the CNT channel in the FET geometry is, for the first time, introduced in order to interpret puzzling findings from several CNT Schottky transistors with asymmetric source and drain contacts.

KEYWORDS: carbon nanotube · nanoscale contacts · passivation · Schottky barrier

Metal/semiconductor contacts play a crucial role in many electronic devices, such as Schottky diodes, metal−semiconductor field-effect transistors (MESFETs), photodetectors, solar cells, *etc*. In the simplest picture, the Schottky barrier (SB) exits at the contact interface between a semiconductor and metal, and the energy barrier height is mainly determined by the difference between the metal work function and semiconductor affinity. However, much more complexity and uncertainty could arise at a nanoscale contact junction, where only a few metal atoms could form the contact and the actual SB height can no longer infer from the traditional contact properties of the metals and semiconductors. To study the properties of nanocontacts, carbon nanotube field-effect transistors (CNTFETs)[1,2] are used as an excellent platform. The nanometer-scaled contacts in CNTFETs do dominate the electrical properties of the devices. Most of CNTFETs exhibit p-type characteristics in ambient conditions without any intentional doping. While early studies suggested hole doping from oxygen,[3,4] it is now generally believed that the CNT/metal contacts play a dominant role. If the Fermi levels of the electrode metals lie below the mid-energy gap of the CNT, a small SB for holes (but large SB for electrons) should form and p-type conduction must be observed. Interestingly, the work function of the electrode metals is found to be strongly affected by adsorbed oxygen. By annealing the CNTFETs in vacuum or desorbing O_2 from the electrodes, the work function of the metal pads decreases so that a small SB for electrons and a large SB for holes are established and a p-type to n-type conversion is achieved.[5,6] Although well-accepted, the above picture is from a common concept for bulk semiconductor/metal contact. It is insufficient to interpret the nature of the nanoscale contacts, especially when the contact area becomes so small that interface adsorbents could affect the contact properties significantly. For this purpose, Yamada first proposed a non-intimate Schottky model in which an interface layer of charged or polarizable molecules is introduced between the CNT/Au contact, which could disturb the charge balance across the contact and modulate the SB.[7,8] Yamada's model presents a physical picture for an individual CNT/metal contact or CNTFETs with symmetric contacts under the influence of environmental oxygen. However, for CNTFETs with asymmetric contacts, especially for CNT-based Schottky diodes, the two different contacts play different roles in determining the device performance, while most importantly, they must interact each other.

Here, for the first time, we propose a concept of "dipole polarization" along the CNT channels. With this concept, the electrostatic charge balance in the entire CNT channel and two contacts is established and, thus, the energy band bending near

*Address correspondence to eqzhang@ntu.edu.sg.

Received for review September 19, 2009 and accepted November 3, 2009.

Published online November 6, 2009.
10.1021/nn9012516

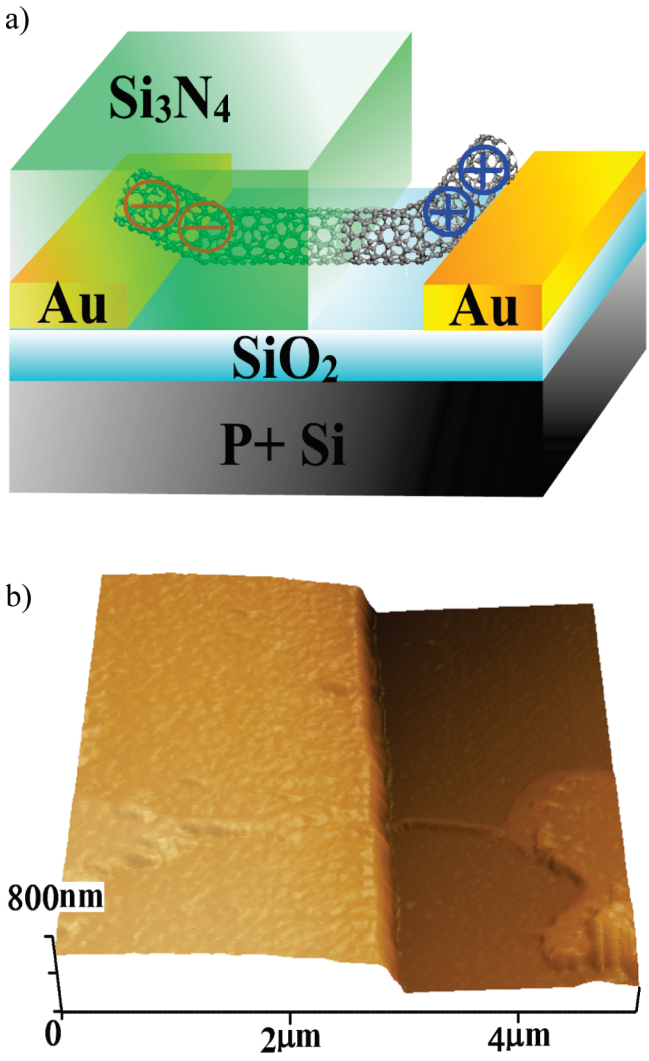

Figure 1. (a) Schematic of a CNTFET with source contact passivated by Si_3N_4. The charges induced in CNTs are illustrated. (b) AFM image of the CNTFET with the source side passivated by Si_3N_4.

the two CNT/metal contacts can be obtained quantitatively. With these understandings, we are able to link the contact properties with the device performance and interpret the unique observations from CNTFETs with asymmetric contact configurations.

RESULTS AND DISCUSSION

Figure 1a illustrates the device structure of a CNTFET with the source contact fully passivated by a Si_3N_4 thin film, while the drain is exposed to air. The atomic force microscope (AFM) image of the actual device is shown in Figure 1b. The asymmetric output characteristics of the device in air are shown in Figure 2. At $V_{GS} = -4$ V, the device shows a higher channel conductance at a positive V_{DS} than that at $-|V_{DS}|$, and the maximum current rectification ratio is more than 10^2. When $V_{GS} = 4$ V is applied, the polarity of the device is flipped. These observations suggest that the device functions as a tunable diode through the gate voltages. More interestingly, the conduction type of the device under $V_{DS} < 0$ is dependent on V_{DS}. As shown in the inset of Figure 2, a

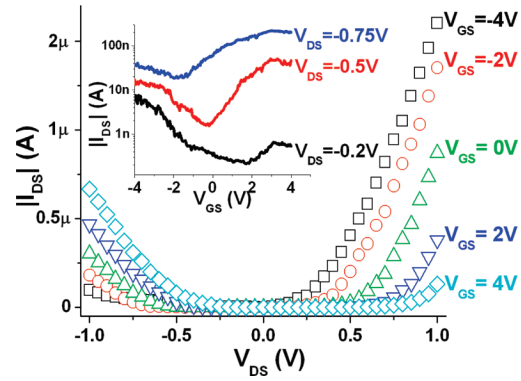

Figure 2. Output characteristics of the CNTFET in atmosphere. Inset: Transfer characteristics of the device under three V_{DS}.

clear p-type to n-type conversion is observed when V_{DS} is varied from −0.2 to −0.75 V. Surprisingly, after the device was placed in vacuum, the n-type behavior, instead of being enhanced, was weakened and the output characteristic became more symmetric (see Supporting Information, Figure S1a). From conventional understandings, the environmental oxygen could cause hole doping to the CNT or increase the electrode metal work function. When the oxygen molecules desorb from the CNT device in vacuum, we would observe n-type instead of p-type conduction. In this sense, the role of oxygen needs to be reconsidered. Yamada suggested that electrostatic charge balance at non-intimate CNT/Au contact can be dominated by adsorbed oxygen.[7] In our devices, the CNTs were manipulated onto predefined Au electrodes.[9,10] Due to the surface roughness of the electrodes, a small gap L (~1 nm) between the Au and CNT could exist, such that a non-intimate Schottky contact is likely to form and the contact SB is susceptible to adsorbed oxygen. In addition to the interface oxygen layer, we find that dipole polarization along the CNT channel must be considered to establish the electrostatic charge balance of the whole device, from one contact to the CNT, and to the other contact. The main purpose here is to study the charge redistribution in the device upon oxygen adsorption. The energy band of the CNT near the contacts must adjust accordingly to restore the charge balance.

In the following, a quantitative picture is obtained by analyzing the energy band bending (EBB) under the influence of the adsorbed oxygen molecules. Note that, even for a top contact configuration with CNT underneath metal electrodes, the charge balance could be still affected by oxygen molecules adsorbed along the contact interface, of course, in a less significant way as compared to the bottom contact configurations.

The single-walled CNTs used in this work have a typical diameter of 1.4 nm. Therefore, the CNTs with a Fermi level of 4.7 eV and a band gap E_g of 0.6 eV are considered in our model. The potential drop across the nanogap ΔU, the CNT electron affinity ϕ_0, Fermi level position ζ (measured from the conduction band edge to the

Fermi level of CNT), surface band bending, and depletion width at the source and drain ($\phi_{S,S}$, $\phi_{S,D}$, W_S, W_D) are marked in Figure 3. Our devices showed an ambipolar characteristic with higher hole conduction under high vacuum (see Supporting Information, Figure S1b), implying that the Fermi level of the Au should align slightly below the midgap of the CNT. Therefore, the effective work function of Au $\chi_m = 4.75$ eV[11−13] is assigned under vacuum conditions in our model.

For the unpassivated drain contact, environmental oxygen molecules adsorbed on the Au surface could easily become negatively charged.[14] Thus, positive charges are induced in Au electrode (σ_m) and CNT (σ_{NT}) to balance these negative oxygen charges (σ_{ox}). The charge neutrality condition can be expressed as follows:

$$\sigma_m + \sigma_{NT} + \sigma_{ox} = 0 \quad (1)$$

In eq 1, $\sigma_m = (\Delta U \varepsilon_g)/(qL)$, where q is the unit charge and ε_g is the permittivity of the gap (since the dielectric constant of gases are close to unity, $\varepsilon_g \approx \varepsilon_0$) and $\Delta U = \phi_S + \phi_0 + \zeta - \chi_m$ is as shown in Figure 3a. The charge supplied by the CNT σ_{NT} can be modeled as $\sigma_{NT} = \pm(2\varepsilon_{NT}|\phi_S|N_B)^{1/2}$, where the permittivity of semiconducting SWNT (s-CNT) $\varepsilon_{NT} \sim 3\varepsilon_0$.[15] The effective doping level can be determined by

$$N_B \sim N_i \exp\frac{\left|\zeta - \frac{1}{2}E_g + \varphi_S\right|}{kT}$$

where k is the Boltzmann constant, T is the absolute temperature, and N_i is the intrinsic carrier density in the CNT ($\sim 10^{22}$ m^{-3}).[16] The influence of the gate modulation on the Fermi level can be modeled as $\zeta = \zeta_0 - \alpha V_G$, where ζ_0 is the Fermi level position at $V_{GS} = 0$ V and the gate efficiency α measures how much gate voltage can move the CNT Fermi level, which is usually less than 0.1 in experiments.[1,2] Considering our back gate structure and thick gate oxide (200 nm SiO_2), we assign $\alpha \sim 0.025$, corresponding to the CNT Fermi level moving from 0.1 eV below midgap to 0.1 eV above, when the gate voltage is swept from −4 to 4 V. Oxygen charge σ_{ox} is given by

$$\sigma_{ox} = -\frac{qP_{O_2}N_A L}{22.4 \times 10^{-3}}$$

where P_{O_2} is the partial pressure of oxygen in atmosphere and N_A is the Avogadro constant.

Solving eq 1 by iteration for ϕ_S, we are now able to depict the detailed EBB. As shown in Figure 3b, a surface band bending at the drain $\phi_{S,D} \approx 0.1$ eV (bending upward from the CNT to Au) with a depletion width

$$W_D = \sqrt{\frac{2\varepsilon_{NT}\varphi_S}{q^2 N_B}} \approx 9.3 \text{ nm}$$

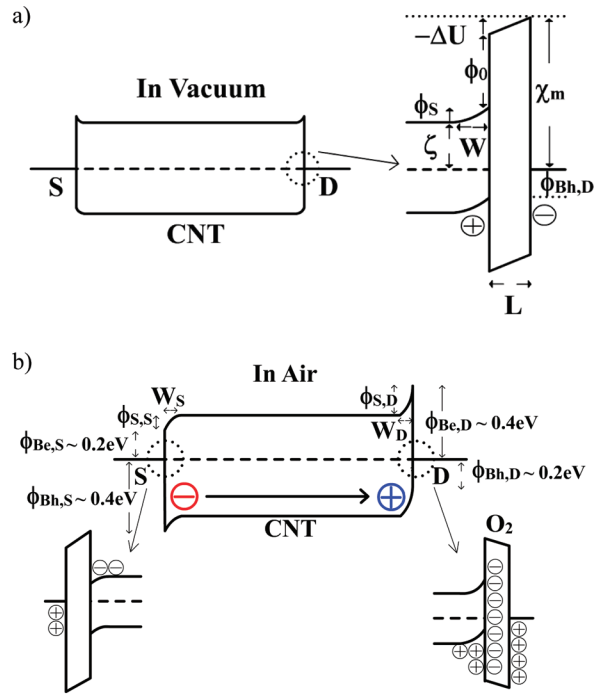

Figure 3. Schematic energy band diagrams of the CNTFET at $V_{DS} = 0$ V and $V_{GS} = 0$ V. (a) Under vacuum and (b) in air.

occurs under $V_{GS} = 0$ V. The Schottky barrier for holes $\phi_{Bh,D} = 1/2E_g - \phi_S = 0.20$ eV is thus obtained. Equivalently, the effective work function of the drain electrode is increased by 0.05 eV under the influence of adsorbed oxygen.

At the source side, the contact is passivated from environmental oxygen by a dense Si_3N_4 layer. Once positive charges are induced at the drain end, the CNT is easily polarized and an electrical dipole should form. According to the first principle calculations, for an s-CNT in our experiment, typically about 95% of the charges are balanced in the longitudinal direction and only 5% are along the radical direction.[17] In other words, negative charges should be induced at the source end. Therefore, static charges are separated at the two ends of CNT, and we name this effect "dipole polarization", which is defined by the product of electrical charges at the two contacts and the distance of them. Using this concept, the electrostatic change balance of the whole system (drain contact−CNT−source contact) is established and the device performance can be predicted. In this case, we have $\sigma_{NT,S} \approx 0.95 \times \sigma_{NT,D} \approx 6 \times 10^{-4}$ C/m^2, and the dipole along the CNT is estimated by $P = \sigma_{NT,S} \times A \times S$, where A is the contact area and the charge separation S is determined by the channel length of the CNTFET (~ 3 μm). From a first-order estimation, we obtain $P \approx 10^{-24}$ C · m. Meanwhile, $\phi_{S,S} \approx -0.10$ eV (bending downward from CNT to Au), $W_S \approx 9.6$ nm, $\phi_{Bh,S} = 0.40$ eV and $\phi_{Be,S} = 0.20$ eV can be obtained for the source contact under $V_{GS} = 0$ V and $V_{DS} = 0$.

Now the p-to-n conversion can be understood through the picture of EBBs. Under negative V_{DS} or V_D

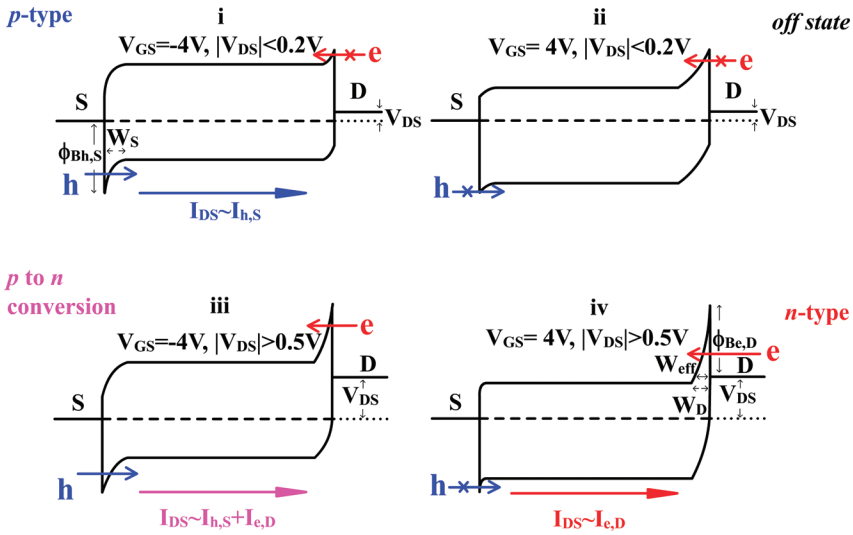

Figure 4. Schematic energy band diagrams in air. (i) $V_{GS} = -4$ V and $|V_{DS}| < 0.2$ V; (ii) $V_{GS} = 4$ V and $|V_{DS}| < 0.2$ V; (iii) $V_{GS} = -4$ V and $|V_{DS}| > 0.5$ V; (iv) $V_{GS} = 4$ V and $|V_{DS}| > 0.5$ V.

$-V_S < 0$, the conduction type is mainly determined by competition between hole current from the source contact and electron current from the drain contact. The highest hole current occurs when holes are injected from the source contact at $V_{GS} = -4$ V, and the hole barrier $\phi_{Bh,S}$ is calculated to be 0.35e V with a length $W_S \approx 26.0$ nm. Similarly, at the maximum electron current ($V_{GS} = 4$ V), the electron barrier $\phi_{Be,D} \approx 0.38$ eV, and $W_D \approx 15.9$ nm are obtained at the drain. Obviously, electrons from the drain encounter a higher but narrower barrier as compared to holes from the source. When the applied $|V_{DS}|$ is small, hole injection at the source contact is favored (see Figure 4i), and the device exhibits p-type behavior. As the magnitude of V_{DS} increases, the effective electron barrier width would become even narrower ($W_{eff} < W_D$). As illustrated in Figure 4iv, when electron tunneling through the drain barrier dominates the current, the transfer characteristic becomes n-type. Our results suggest that both V_{DS} and V_{GS} could affect the EBB which controls the carrier transport through the contacts.

In our device discussed above, oxygen induces an upward bending at the unpassivated drain contact, which allows electron tunneling at largely negative V_{DS}. Meanwhile, the polarization along the CNT increases the SB height for holes in the passivated source contact. As a result, n-type conduction is observed in air. Once the adsorbed oxygen is removed from the drain contact in vacuum, the polarization effect fades away and the hole injection from the source contact is no longer suppressed. Thus, the device exhibits an ambipolar characteristic with stronger hole conduction. In contrast, for CNTFETs with Au and Ti[18] or Pd and Al[19] top contacts in air, as oxygen molecules adsorb at both the source and drain contacts, no polarization along CNT would occur. Due to the negative charges from oxygen molecules, the hole SBs are lowered at both contacts, leading to enhancement of hole conduction. As a result, n-type characteristics were not observed in air. For comparison, we fabricated a Schottky FET with Au and Al contacts, in which the CNT was placed on top of the Au electrode on one side (bottom contact) and embedded inside the Al contact on the other side (top contact).[20] The device exhibited n-type characteristics under vacuum, implying the electron SB is smaller at the Al contact than hole SB at the Au contact. After it was placed in air, oxygen could reduce the SB height for hole at the Au contact. However, since the CNT/Al intimate contact is less affected by oxygen as compared to the CNT/Au contact, the dipole polarization could still occur along the CNT and the SB height for electrons at the Al contact is lowered. As a result, the n-type performance remained in ambient conditions (see Supporting Information for details).

CONCLUSION

In summary, we have developed a novel model for CNT/metal contacts, in which the electrostatic charge balance across the contact and the dipole polarization along the CNT are appropriately taken into consideration. Our model shows that, under the influence of the negative charges from adsorbed oxygen molecules at the interface, an upward band bending is induced in the CNT or, in other words, the work function of the metal electrodes is effectively increased. Only for those CNTFETs with one of the two CNT/metal contacts protected, the dipole polarization effect can be observed and becomes important in determining the conduction type of the devices.

MATERIALS AND METHODS

SWNT Suspension. Highly purified SWNTs were dispersed in deionized water with 1 wt % Triton X-100. After ultrasonic agitation using a tip-sonicator (MISONIX sonicator 3000) at a power of 480 W/L for 2 min, the suspension was centrifuged (SIGMA sartorius 2−16) at 6461*g* for 2 h. Then, the upper 30% supernatant was carefully decanted. The suspension was then ultrasonically agitated for more than 30 min.

Device Fabrication. The well-dispersed SWNT suspension was introduced to patterned Au/Ti electrodes on a heavily doped p-type silicon wafer with a 200 nm SiO_2 layer on top. An ac voltage with a 6 MHz frequency was then applied across the electrodes. The peak-to-peak voltage was selected in the range of 6 to 10 V, depending on the electrode separation. Confirmation for bridging CNTs between the electrodes can be done by monitoring the resistance across. After an SWNT was placed across the

electrodes, the device was placed at 10^{-7} Torr overnight, so that adsorbed gas molecules could desorb. A 500 nm thick Si_3N_4 layer was then selectively deposited to passivate the entire source contact area, using mixed flow gases of 100 sccm 4% diluted silane gas, 20 sccm ammonia gas, and 600 sccm nitrogen gas at 50 °C with 40 W rf power.

Acknowledgment. We thank the MOE AcRF Tier 2 Funding (ARC17/07, T207B1203) for generous support. N.P. would like to acknowledge the Chartered-NTU graduate research scholarship.

Supporting Information Available: Device performance under vacuum, Schottky diode with Au and Al contacts. This material is available free of charge *via* the Internet at http://pubs.acs.org.

REFERENCES AND NOTES

1. Tans, S. J.; Verschueren, A. R. M.; Dekker, C. Room-Temperature Transistor Based on a Single Carbon Nanotube. *Science* **1998**, *397*, 49–52.
2. Martel, R.; Schmidt, T.; Shea, H. R.; Hertel, T.; Avouris, Ph. Single- and Multi-Wall Carbon Nanotube Field-Effect Transistors. *Appl. Phys. Lett.* **1998**, *73*, 2447–2449.
3. Collins, P. G.; Bradley, K.; Ishigami, M.; Zettl, A. Extreme Oxygen Sensitivity of Electronic Properties of Carbon Nanotubes. *Science* **2000**, *287*, 1801–1804.
4. Jhi, S.-H.; Louie, S. G.; Cohen, M. L. Electronic Properties of Oxidized Carbon Nanotubes. *Phys. Rev. Lett.* **2000**, *82*, 1710–1713.
5. Derycke, V.; Martel, R.; Appenzeller, J.; Avouris, Ph. Controlling Doping and Carrier Injection in Carbon Nanotube Transistors. *Appl. Phys. Lett.* **2002**, *80*, 2773–2775.
6. Heinze, S.; Tersoff, J.; Martel, R.; Derycke, V.; Appenzeller, J.; Avouris, Ph. Carbon Nanotube as Schottky Barrier Transistors. *Phys. Rev. Lett.* **2002**, *89*, 106801-1–106801-4.
7. Yamada, T. Modeling of Carbon Nanotube Schottky Barrier Modulation under Oxidizing Conditions. *Phys. Rev. B* **2004**, *69*, 125408-1–125408-8.
8. Yamada, T. Equivalent Circuit Model for Carbon Nanotube Schottky Barrier: Influence of Neutral Polarizaed Gas Molecules. *Appl. Phys. Lett.* **2006**, *88*, 083106-1–083106-3.
9. Li, J.; Zhang, Q.; Peng, N.; Zhu, Q. Manipulation of Carbon Nanotubes Using AC Dielectrophoresis. *Appl. Phys. Lett.* **2005**, *86*, 153116-1–153116-3.
10. Peng, N.; Zhang, Q.; Li, J.; Liu, N. Influence of Ac Electric Field on the Spatial Distribution of Carbon Nanotubes Formed between Electrodes. *J. Appl. Phys.* **2006**, *100*, 024309-1–024309-5.
11. Michaelson, H. B. The Work Function of the Elements and Its Periodicity. *J. Appl. Phys.* **1977**, *48*, 4729–4733.
12. Ishii, H.; Sugiyama, J.; Ito, E.; Seki, K. Energy Level Alignment and Interfacial Electronic Structures at Organic/Metal and Organic/Organic Interfaces. *Adv. Mater.* **2009**, *11*, 605–625.
13. Cui, X.; Freitag, M.; Martel, R.; Brus, L.; Avouris, Ph. Controlling Energy-Level Alignments at Carbon Nanotube/Au Contacts. *Nano Lett.* **2003**, *3*, 783–787.
14. Mills, G.; Gordon, M. S.; Metiu, H. Oxygen Adsorption on Au Clusters and a Rough Au(111) Surface: The Role of Surface Flatness, Electron Confinement, Excess Electrons, and Band Gap. *J. Chem. Phys.* **2003**, *118*, 4198–4205.
15. Benedict, L. X.; Louie, S. G.; Cohen, M. L. Static Polarizabilities of Single-Wall Carbon Nanotubes. *Phys. Rev. B* **1995**, *52*, 8541–8549.
16. Marulanda, J. M.; Srivastava, A. Carrier Density and Effective Mass Calculations in Carbon Nanotubes. *Phys. Status Solidi B* **2008**, *245*, 2558–2562.
17. Kozinsky, B.; Marzari, N. Static Dielectric Properties of Carbon Nanotubes from First Principles. *Phys. Rev. Lett.* **2006**, *96*, 166801-1–166801-4.
18. Yang, M. H.; Teo, K. B. K.; Milne, W. I.; Hasko, D. G. Carbon Nanotube Schottky Diode and Directionally Dependent Field-Effect Transistor Using Asymmetrical Contacts. *Appl. Phys. Lett.* **2005**, *87*, 253116-1–253116-3.
19. Lu, C.; An, L.; Fu, Q.; Liu, J.; Zhang, H.; Murduck, J. Schottky Diodes from Asymmetric Metal-Nanotube Contacts. *J. Appl. Phys. Lett* **2006**, *88*, 133501-1–133501-3.
20. Li, H.; Zhang, Q.; Marzari, N. Unique Carbon-Nanotube Field-Effect Transistors with Asymmetric Source and Drain Contacts. *Nano Lett.* **2008**, *8*, 64–68.